

# Long-lifetime green-emitting Tb<sup>3+</sup> complexes for bacterial staining

Weronika Rochowiak<sup>A</sup>, Ewa Kasprzycka<sup>A,C</sup>, Israel P. Assunção<sup>A,D</sup>, Ulrich Kynast<sup>A,\*</sup>  and Marina Lezhnina<sup>B,\*</sup>

For full list of author affiliations and declarations see end of paper

**\*Correspondence to:**

Ulrich Kynast, Marina Lezhnina  
 Muenster University of Applied Sciences,  
 Institute for Optical Technologies,  
 Stegerwaldstr. 39, 48565 Steinfurt,  
 Germany  
 Email: [uk@fh-muenster.de](mailto:uk@fh-muenster.de),  
[marina@fh-muenster.de](mailto:marina@fh-muenster.de)

**Handling Editor:**

George Koutsantonis

**Received:** 1 December 2021

**Accepted:** 18 February 2022

**Published:** 18 May 2022

**Cite this:**

Rochowiak W *et al.* (2022)  
*Australian Journal of Chemistry*  
**75**(8 & 9), 754–759. doi:[10.1071/CH21315](https://doi.org/10.1071/CH21315)

© 2022 The Author(s) (or their employer(s)). Published by CSIRO Publishing.

This is an open access article distributed under the Creative Commons Attribution-NonCommercial-NoDerivatives 4.0 International License ([CC BY-NC-ND](https://creativecommons.org/licenses/by-nc-nd/4.0/))

OPEN ACCESS

## ABSTRACT

The present report describes a new approach to stain bacteria by means of rare earth complexes. We demonstrate with selected Gram-negative and positive bacteria (*Escherichia coli*, *Micrococcus luteus*, *Bacillus megaterium*) that these microbes can be stained efficiently with derivatives of *N*-phenyl-anthranilic acid, flufenamic acid in particular, and Tb<sup>3+</sup> ions. Hence, the inherent advantages of rare earth complexes, e.g. strong optical absorption (>50 000 L × M<sup>-1</sup> × cm<sup>-1</sup>) due to the antenna effect, large Stokes' shifts (~10 000 cm<sup>-1</sup>) and very long emission decay times (millisecond range), and, not least, enhanced photostability can be fully exploited in fluorescence microscopy and spectroscopy of the bacteria; foreseeably, these findings will also be useful in flow cytometry and ELISA techniques.

**Keywords:** bacteria, fluorescence microscopy, lifetime, luminescence, rare earth complexes, staining.

## Introduction

In the context of microbes, rare earth ions have scarcely been studied. Only a few reports are devoted to 'direct' rare earth stains for bacteria and spores,<sup>[1–4]</sup> the term 'direct bacterial staining' referring to simple procedures as known for 'classical' organic cell dyes like Sybr Green (SG) or propidium iodide (PI).<sup>[5]</sup> Often, these essentially just require the incubation of the bacterial suspensions with the dye. In contrast to that and larger in number, rare earth-based techniques predominantly employ 'indirect' staining techniques, i.e. aim at liberated bacterial DNA, other secreted biomolecules, or dedicated antibodies, which have been shown to be useful in several bioanalytical and immunological methods, like polymerase chain reaction (PCR), enzyme-linked immunosorbent assay (ELISA), fluorescence flow cytometry and lateral flow assays.<sup>[6–14]</sup> However, these indirect methods require tedious and time-consuming preliminary preparations of, for example, antibodies, fairly costly equipment and highly skilled personnel.

The intrinsic optical properties of Tb<sup>3+</sup> ions, the focus here, arise from the nature of the *f*-orbitals: on one hand, their screening from the chemical environment advantageously leads to very narrow *f*–*f* excitation and emission lines, while the quantum mechanically forbidden nature of *f*–*f* transitions effect long decay times (ms) of the excited *f*-states, but also to disadvantageously weak absorption intensities on the other hand. To cope with the poor *f*–*f* absorptivity viz excitability in the bio-analytically relevant spectral range above 300 nm, the 'antenna-effect' is used to sensitize Tb<sup>3+</sup>. Numerous articles and reviews outline the mechanisms involved and their benefits for bio-analytics, just three of which, covering mechanisms, biomedical applications and some economical aspects are quoted here.<sup>[15–17]</sup> In brief, a suitable ligand with allowed, strong and comparably broad absorptions in the relevant spectral range forms a complex with the Tb<sup>3+</sup> ion; after excitation of the ligand (<sup>1</sup>S<sub>0</sub> → <sup>1</sup>S\*), it undergoes inter-system crossing into an associated triplet state (<sup>1</sup>S\* → <sup>3</sup>T, enabled by spin–orbit coupling), from which the energy is transferred radiationlessly to energetically close Tb<sup>3+</sup> states. Finally, characteristic Tb<sup>3+</sup> emissions will typically occur from the excited <sup>5</sup>D<sub>4</sub> state of Tb<sup>3+</sup>. The process is limited by the ligands'

triplet energies, which have to be located at least  $2000\text{ cm}^{-1}$  above the emitting  $^5\text{D}_4$ -level ( $20\,500\text{ cm}^{-1}$ ) to prevent back-transfer into the ligand's  $^3\text{T}$  level.<sup>[18,19]</sup> A most important complex described in the past is tri-anionic tris(pyridine-2,6-dicarboxylato)terbium,  $[\text{Tb}((\text{C}_5\text{H}_4\text{N})(\text{COO})_2)_3]^{3-}$  (also referred to as  $[\text{Tb}(\text{dipicolinate})_3]^{3-}$  or  $[\text{Tb}(\text{dpa})_3]^{3-}$ ),<sup>[20]</sup> especially as a stain for endospores,<sup>[1,21]</sup> though their excitation unfortunately lies in the deep UV below 300 nm.

The abovementioned long decay times can most favourably be used to discriminate the emission signal from other dyes, and the highly problematic autofluorescence in matrices of biological origin in particular (by time-gated luminescence).<sup>[21–23]</sup> The feasibility of using long-lived red-emitting microbe stains based on Eu diketonate complexes has recently been evaluated.<sup>[4]</sup> Furthermore, the narrow-line emissions of  $\text{Tb}^{3+}$ , as well as most other rare earth ions of interest, can be of extreme value where filters have to be used to separate excitation and emission. Combined with the broad excitation bands of the complexes just below 400 nm, i.e. Stokes shifts of more than 150 nm, superb microbial luminescence monitors become available for the photoluminescent applications listed above.

Last but not least, we envisage that rare earth stains hold the promise of superior photostability over purely organic dyes like SG, photobleaching being an omnipresent bottleneck in fluorescence microscopy and flow cytometry.<sup>[24–26]</sup>

## Experimental

### Materials

The ligand, with a purity of  $>98\%$ , was purchased from TCI chemicals (Belgium). For the experiments, ethanolic solutions were prepared and the desired  $\text{TbCl}_3$  ethanolic solutions were prepared from a 100 mM stock solution. The pure complex  $\text{Tb}(\text{fluf})_3$  (fluf = flufenamate) was prepared as described earlier.<sup>[27]</sup>

### Spectroscopy

Emission and excitation spectra as well as luminescence decay of the dispersions were measured on an Edinburgh FS5 spectrofluorometer (180 W Xe lamp, 5 W microsecond Xe flash lamp, cooled and stabilized photomultiplier R928P) at room temperature. The excitation and emission spectra were recorded after centrifugation and re-dispersion of the bacteria in buffer, yielding approximately  $2.4 \times 10^8$  bacteria  $\text{mL}^{-1}$ .

### Microscopy

Microscope images were taken with a Leica DMi8 fluorescence microscope equipped with filtercubes ( $\text{Tb}^{3+}$ : excitation 365 nm, emission 545 nm) and a CoolLED pE-4000 LED light source. The pictures of SG staining were obtained using an FITC filtercube (excitation 460–500 nm, emission

512–542 nm) and for PI staining, a TXR filtercube (excitation 540–580 nm, emission 592–668 nm) was used. The pictures were taken using  $100\times$  and  $63\times$  magnification objectives; the irradiance intensity was set to 30%. The camera exposure time was 130 ms.

### Bacteria

The bacterial strains in this work (DSM 1116, *Escherichia coli*; DSM 20030, *Micrococcus luteus*; DSM 90, *Bacillus megaterium*) were purchased from DSMZ (Leibniz Institute DSMZ; German Collection of Microorganisms and Cell Cultures GmbH, Braunschweig, Germany). The bacterial cultures were taken from tryptic soy agar plates and inoculated into tryptic soy broth (caso bouillon, Merck KGaA, Darmstadt, Germany) to grow overnight. Then the bacteria were centrifuged and redispersed in 50 mM HEPES buffer (pH 7.5) of above 99.5% purity purchased from Sigma-Aldrich.

The approximate numbers of bacteria in samples were calculated using the optical density of the dispersion at 600 nm. The density was measured on a Specord 200 Plus UV-visible spectrophotometer (Analytik Jena) using 1 cm acrylic cuvettes.

Bacterial dispersions in HEPES buffer ( $2.4 \times 10^7$  cells  $\text{mL}^{-1}$ ) were first incubated with 10  $\mu\text{L}$  HFluf (30 mM ethanolic solution, 30 min) followed by treatment with 10  $\mu\text{L}$   $\text{TbCl}_3$  (10 mM ethanolic solution, 30 min).

Staining with the whole complex was done by incubating bacterial dispersions with 10  $\mu\text{L}$  of 30 mM complex dissolved in ethanol for 1–2 h.

## Results and discussion

We recently described a new series of green-emitting  $\text{Tb}^{3+}$  complexes based on derivatives of *N*-phenylanthranilic acid (fenamic acid), with efficiencies up to 33% and decay times of 873  $\mu\text{s}$  for  $\text{Tb}(\text{meclofenamate})_3(\text{H}_2\text{O})_2$  for example.<sup>[27]</sup> The efficiency of the complexes could be greatly enhanced by co-coordination with an ancillary 5,5'-dimethyl-2,2'-bipyridine ligand (5,5'-dmbipy) to yield a quantum efficiency of 60% at a decay time of 1270  $\mu\text{s}$ , this for the complex  $\text{Tb}(\text{flufenamate})_3(5,5'\text{-dmbipy})$  (Fig. 1),<sup>[28]</sup> which

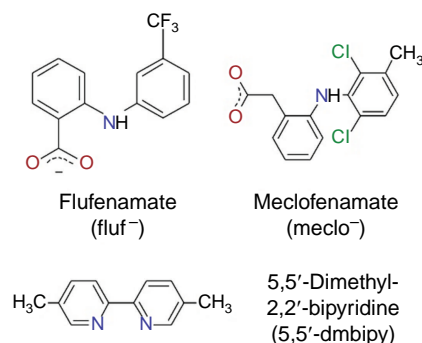


Fig. 1. Ligands for  $\text{Tb}^{3+}$  used in this investigation.

showed the largest gain over the non-co-coordinated complexes. This gain via co-coordination nurtured our hope that the numerous functional groups on or in bacteria would be able to provide an analogous efficiency boost. Indeed, Tb (flufenamate)<sub>3</sub>H<sub>2</sub>O (Tb(fluf)<sub>3</sub>) proved to be the best complex for microbial staining and is the focus of the following discussion. To include the different membrane construction of Gram-negative (thickness of cell wall typically less than 10 nm, lipopolysaccharide surface) and Gram-positive (thickness of cell wall up to 80 nm, containing teichoic acids) bacteria, *Escherichia coli* (Gram-negative), *Micrococcus luteus* and *Bacillus megaterium* (both Gram-positive) were chosen; *B. megaterium* was selected as the largest of these bacteria and is known to readily form spores on stress.<sup>[29]</sup>

Generally, a two-step procedure was pursued: a first step involving incubation with flufenamate (fluf<sup>-</sup>), followed by the addition of Tb<sup>3+</sup> solution as the second step. The fluorescence microscopy images and their overlay with the bright-field images are shown in Fig. 2. Obviously, all bacteria could be stained to give satisfying and bright fluorescence images, staining of *E. coli* working the best owing to its thin cell wall. *M. luteus* is known to form smaller aggregates (tetrads), which seem to agglomerate even further in the presence of Tb<sup>3+</sup>; *B. megaterium* takes up the least stain,

this most likely being related to sporulation, as apparent in Fig. 1 (inset right image and Supplementary Fig. S1).

On plating the fluf<sup>-</sup>/Tb<sup>3+</sup> incubated dispersions on agar plates, all samples formed colonies after 3 days. However, live-dead staining with SG (green emission in live bacteria) and PI (red emission in dead bacteria) revealed an increasing number of dead microbes, as indicated by the dominance of the PI emission from *E. coli* and *B. megaterium* (Supplementary Fig. S2). It should be pointed out, though, that care has to be taken in evaluating the fluorescence images: SG emission and PI absorption exhibit a large spectral overlap and energy transfer fluorescence resonance energy transfer (FRET); hence, the red PI emission can easily be overemphasized and falsify the picture. In the case of *B. megaterium*, no live bacteria were found after staining; however, as pointed out above, this may be related to sporulation.

We also tested bacterial viability by incubating all three species for 0.5, 2 and 24 h in the buffered fluf<sup>-</sup> solution alone with subsequent plating on agar plates; after 3 days, no difference with blanks (bacteria in buffer only) was noted. Additionally, live-dead stains (SG and PI) support the conclusion that the addition of fluf<sup>-</sup> in the first step leaves the bacteria generally intact.

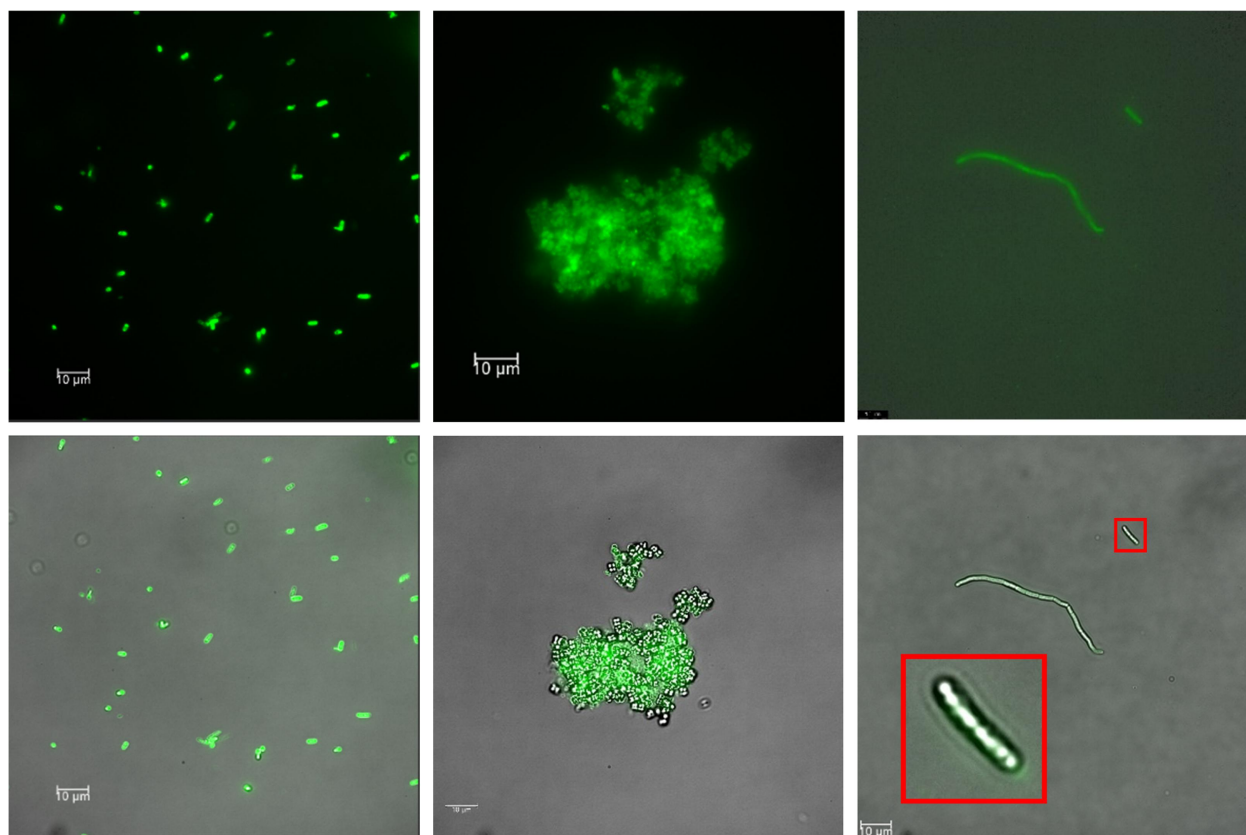


**Fig. 2.** Fluorescence microscopy images of *E. coli* (left, objective lens 63 $\times$ ), *M. luteus* (middle, objective lens 100 $\times$ , scale bar 10) and *B. megaterium* (right, objective lens 63 $\times$ ); excitation 365 nm, emission 545 nm; the scale bar is 10  $\mu$ m in all images. The inset in the overlay of *B. megaterium* shows a pearl-necklet-like alignment of spores.

Furthermore, we evaluated the cytotoxicity of  $\text{Tb}^{3+}$  alone by first incubating the bacteria in buffered  $\text{Tb}^{3+}$  solution. Subsequently, they were plated on agar plates, which revealed growth of all three, although somewhat inhibited in comparison with plated blanks. In parallel, we used SG and PI staining right after the  $\text{Tb}^{3+}$  incubation. Supplementary Fig. S3 shows the presence of predominantly live bacteria, except for *E. coli*, for which a larger number appears to be dead, although the same consideration with regard to SG-PI-FRET as above holds true here as well.

The reverse order of incubation ( $\text{Tb}^{3+}$  followed by addition of  $\text{fluf}^-$ ) led to very similar results with respect to staining intensities in the fluorescence images. Generally, however, the degree of agglomeration is somewhat higher if  $\text{Tb}^{3+}$  incubation is conducted first, which can be ascribed to the fact, well known from colloid chemistry, that trivalent cations are strong coagulants for negatively charged particles.

By the aid of fluorescence microscopy, it is furthermore possible to show that the stains are contained within the cells rather than on the surface alone: cross-section brightness profiles are shown in Fig. 3 for *E. coli* (for other species, see Supplementary Fig. S1). We furthermore took excitation and emission spectra of dispersions of the bacteria and determined the lifetimes of the ingested complexes; again the spectra for *E. coli* displayed in Fig. 4 serve as an example (see Supplementary Fig. S4 for the other species). The excitation maxima are found at  $\sim 365$  nm, which perfectly matches the emission of commercial high-power UV-LEDs, such that fairly low-cost monitoring is accessible; of course, our advanced fluorescence microscope also profits from this coincidence.

We should point out here that, other than suggested by the bright fluorescence image on first sight (Fig. 2, centre row), *M. luteus* unexpectedly had the lowest spectroscopic excitation and emission signals. At the same time, the

luminescence images showed that the complex is also strongly allocated in between the microbes. The emission intensity was clearly the lowest for *M. luteus*; it took several incubation attempts to obtain sufficiently emissive bacteria for recording the lifetimes. We have to concede that we had significant problems with the reproducible growth of *M. luteus* in previous investigations. The reason for this is not completely clear, but may be related to the fact that *M. luteus* lacks a glykokalyx capsule at the outer cell wall, which may promote the uptake of the growth-inhibiting complex on one hand. On the other hand, with respect to luminescence, the yellow carotenoid sarcinaxanthin ( $\lambda_{\text{max}} = 450$  nm), inevitably present in *M. luteus*, readily interferes via its triplet state with the  $\text{Tb}^{3+}$  ion's  $^5\text{D}_4$  f state and decreases its emission. Whether *M. luteus* partly metabolizes the complex, or the capsule is needed for more efficient endocytosis of the complexes is an open question still to be tackled.

The decay times  $\tau_2$  of *E. coli*, *B. megaterium* and *M. luteus* are considerably higher than for the free complex  $\text{Tb}(\text{fluf})_3(\text{H}_2\text{O})$ , especially considering that the free complex was measured as a solid. The true nature of the intracellular complex, e.g. neutral  $[\text{Tb}(\text{fluf})_3]$ , monocationic  $[\text{Tb}(\text{fluf})_2]^+$  or dicationic  $[\text{Tb}(\text{fluf})]^{2+}$ , could not be verified; evidently, however, the complexes are unambiguously linking to coordinating functional groups of the bacteria. The fact that the decays were best fitted as bi-exponentials yielding a comparably short decay  $\tau_1$  is tentatively ascribed to species adhering to the surface of the bacteria, where they are exposed to quenching through the aqueous environment. Near-surface allocated complexes would obviously be in accord with the brightness profiles as well (Table 1).

Somewhat to our surprise, a one-step staining procedure with the complex itself for the Gram-negative *E. coli* (see Supplementary Fig. S5) also led to acceptable results, although at appreciably lower brightness levels. In contrast,

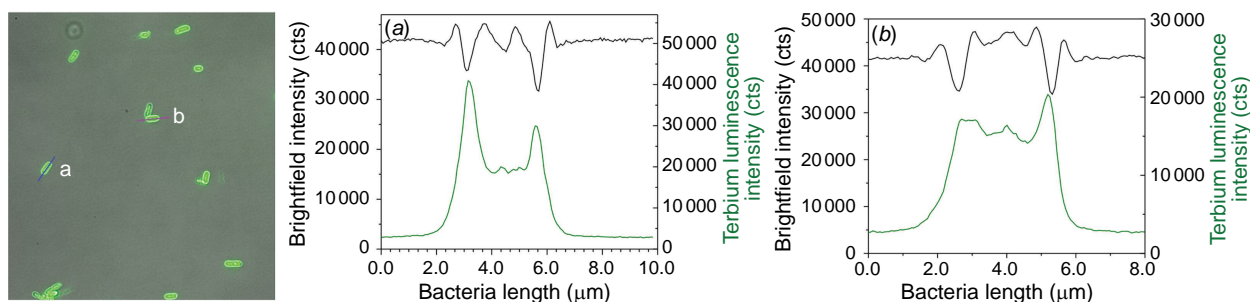


**Fig. 3.** Brightness profiles/cross sections through *E. coli*. The blue (a) and violet (b) lines in the overlay of brightfield and fluorescence channels indicate the measured ranges in micrometres (left image). Plots of the corresponding brightness values (a, b) are depicted in the middle and right graphs. The top black lines show brightness dips for white light at the beginning and the end of the bacteria. At the same time, the bottom green lines indicate the location of the complex along the section. High brightnesses at the edges indicate that there may be a higher concentration in surface areas, enhanced by the stronger absorption, i.e. longer passage of the exciting light, at the edges. Significantly, the brightness levels (cts, counts) throughout the bacteria are far above the background levels.

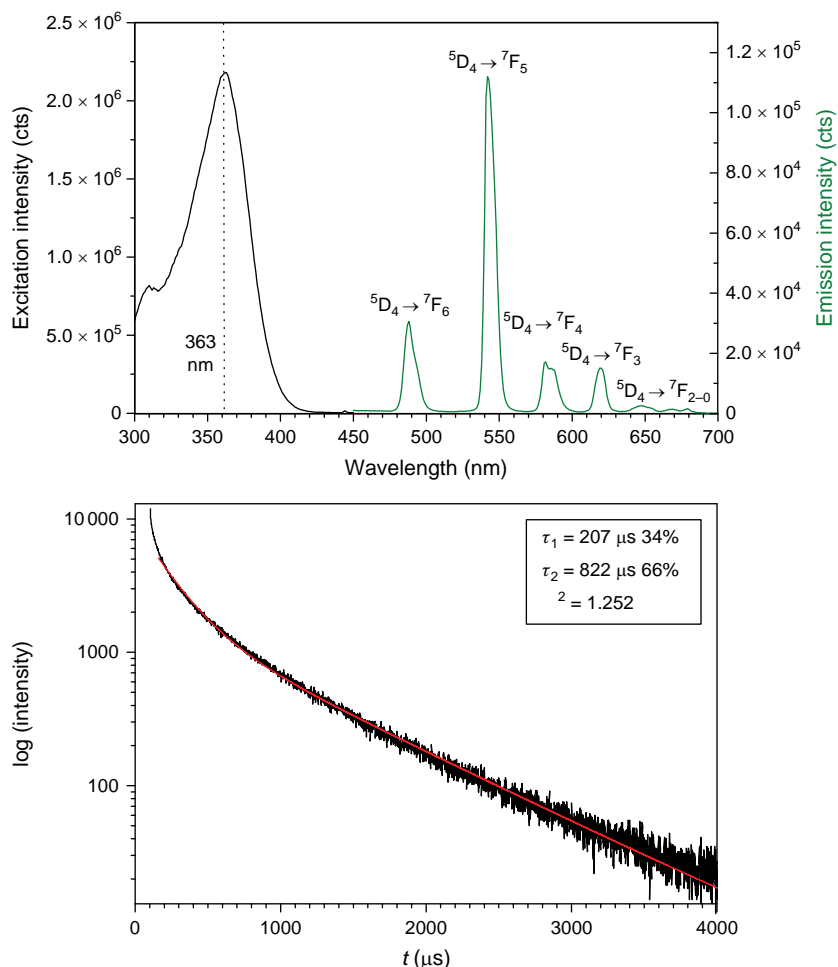


**Fig. 4.** Excitation and emission spectra (top), and decay curves (bottom) from dispersions of the stained *E. coli* ( $\tau_1$  and  $\tau_2$ : decay components of the bi-exponential fit,  $\chi^2$ : goodness of fit).

**Table I.** Spectral data of  $\text{Tb}^{3+}$  species in this investigation; percentages of first and second order decays in parentheses.

Species	$\text{Tb}(\text{fluf})_3(\text{H}_2\text{O})$ , solid <sup>[27]</sup>	$\text{Tb}(\text{fluf})_3(5,5'\text{-dmbp})$ , solid <sup>[28]</sup>	$\text{Tb}^{3+}$ <i>E. coli</i>	$\text{Tb}(\text{fluf})_3^{\text{A}}$ <i>E. coli</i>	$\text{Tb}(\text{fluf})_3^{\text{A}}$ <i>M.</i> <i>luteus</i>	$\text{Tb}(\text{fluf})_3^{\text{A}}$ <i>B.</i> <i>megaterium</i>
Decay time $\tau_1$ ( $\mu\text{s}$ )				207 (34%)	85 (18%)	170 (31%)
Decay time $\tau_2$ ( $\mu\text{s}$ )	434	1275	283	822 (66%)	459 (82%)	700 (84%)
Maximum excitation (nm)	365	375	290	363	365	363

<sup>A</sup>In the bacteria, the complexes may be cationic, e.g.  $[\text{Tb}(\text{fluf})_2]^+$ ; see text.

the Gram-positive bacterial cells did not respond to the whole complex as such; instead, the complex precipitated from the dispersion in the vicinity of the bacteria. This observation again corroborates the role of the thinner cell walls of the Gram-negative bacteria. It is conceivable that via this pathway a simple alternative Gram stain can be devised.

Last but not least,  $\text{Tb}(\text{fluf})_3$  in the bacteria proved to be far more stable photochemically than SG (half-life 69 vs 17 s), which motivates us to conduct further systematic studies on this issue.

## Conclusions

We have demonstrated for the first time that green-emitting Tb complexes with highly desired excitation in the spectral range above 350 nm can be used as efficient luminescent stains for bacteria, Gram-negative bacteria (*E. coli*) yielding greater brightness in the fluorescence images than Gram-positives, which can be attributed to the thickness of the cell walls. The predominant luminescence lifetimes of up to approximately 800  $\mu\text{s}$  in the aqueous bacteria dispersions, by far in excess of the free complexes, show the synergistic

interaction with functional groups of the bacteria. The long lifetimes will be an indispensable asset, exploitable in time-gating analyses such as luminescent flow cytometry and time gated microscopy. Furthermore, although yet to be detailed for other organic dyes, the photostability of the bacterial complexes was shown to outshine SG as a prominent example for an organic dye.

## Supplementary material

Supplementary material is available [online](#) consisting of supplementary Figs S1–S5 with additional microscopic images, excitation and emission spectra, decay curves and brightness profiles.

## References

- [1] Pellegrino PM, Fell NF, Rosen DL, Gillespie JB. *Anal Chem* 1998; 70: 1755–1760. doi:10.1021/ac971232s
- [2] Rosen DL, Sharpless C, McGown LB. *Anal Chem* 1997; 69: 1082–1085. doi:10.1021/ac960939w
- [3] Högmander M, Paul CJ, Chan S, Hokkanen E, Eskonen V, Pahikkala T, Pihlasalo S. *Anal Chem* 2017; 89: 3208–3216. doi:10.1021/acs.analchem.6b05142
- [4] Lezhnina MM, Rochowiak W, Göhde W, Kuczius R, Kynast U. *J Biophotonics* 2020; 13: e202000068. doi:10.1002/jbio.202000068
- [5] Sabnis RW. *Handbook of biological dyes and stains: synthesis and industrial applications*. John Wiley & Sons; 2010.
- [6] Hagren V, von Lode P, Syrjäälä A, Soukka T, Lövgren T, Kojola H, Nurmi J. *Anal Biochem* 2008; 374: 411–416. doi:10.1016/j.ab.2007.12.017
- [7] Dasch GA, Halle S, Bourgeois AL. *J Clin Microbiol* 1979; 9: 38–48. doi:10.1128/jcm.9.1.38-48.1979
- [8] Jin D. Background-free Cytometry Using Rare Earth Complex Bioprobes in: Darzynkiewicz Z, Holden E, Orfao A, Telford W, Wlodkowic D, editors. *Methods in Cell Biology*. Academic Press; 2011. Vol. 102, pp. 479–513.
- [9] Jin D, Piper JA, Leif RC, Yang S, Ferrari BC, Yuan J, Wang G, Vallarino LM, Williams JW. *J Biomed Opt* 2009; 14: 024023. doi:10.1117/1.3103770
- [10] Gordon J, Michel G. *Clin Chem* 2008; 54: 1250–1251. doi:10.1373/clinchem.2007.102491
- [11] Ham JY, Jung J, Hwang B-G, Kim W-J, Kim Y-S, Kim E-J, Cho M-Y, Hwang M-S, Won DI, Suh JS. *Ann Lab Med* 2015; 35: 50–56.
- [12] Nurmi J, Wikman T, Karp M, Lövgren T. *Anal Chem* 2002; 74: 3525–3532. doi:10.1021/ac020093y
- [13] Zhang P, Liu X, Wang C, Zhao Y, Hua F, Li C, Yang R, Zhou L. *PLoS One* 2014; 9: e105305. doi:10.1371/journal.pone.0105305
- [14] Matsumoto K. In: Bünzli J-CG, Pecharsky VK, editors. *Handbook on the Physics and Chemistry of Rare Earths*. Elsevier; 2020; Vol. 57, pp. 119–191.
- [15] Bünzli J-CG. *Coord Chem Rev* 2015; 293-294: 19–47. doi:10.1016/j.ccr.2014.10.013
- [16] Selvin PR. *Annu Rev Biophys Biomol Struct* 2002; 31: 275–302. doi:10.1146/annurev.biophys.31.101101.140927
- [17] Bünzli J-CG. *J Lumin* 2016; 170: 866–878. doi:10.1016/j.jlumin.2015.07.033
- [18] Latva M, Takalo H, Mukkala V-M, Matachescu C, Rodríguez-Ubis JC, Kankare J. *J Lumin* 1997; 75: 149–169. doi:10.1016/S0022-2313(97)00113-0
- [19] Bünzli J-CG. Rare Earth Luminescent Centers in Organic and Biochemical Compounds in: Hull R, Parisi J, Osgood RM, Warlimont H, Liu G, Jacquier B, editors. *Spectroscopic Properties of Rare Earths in Optical Materials*. Berlin, Heidelberg: Springer; 2005. pp. 462–499.
- [20] Chauvin A-S, Gummy F, Imbert D, Bünzli J-CG. *Spectrosc Lett* 2004; 37: 517–532. doi:10.1081/SL-120039700
- [21] Zhang KY, Yu Q, Wei H, Liu S, Zhao Q, Huang W. *Chem Rev* 2018; 118: 1770–1839. doi:10.1021/acs.chemrev.7b00425
- [22] Sayyadi N, Connally RE, Lawson TS, Yuan J, Packer NH, Piper JA. *Molecules* 2019; 24: 2083. doi:10.3390/molecules24112083
- [23] Garcia-Fernandez E, Pernagallo S, González-Vera JA, Ruedas-Rama MJ, Díaz-Mochón JJ, Orte A. In: Pedras B, editor. *Fluorescence in Industry*. Cham: Springer International Publishing; 2019. pp. 213–267.
- [24] Tajiri K, Kishi H, Ozawa T, Sugiyama T, Muraguchi A. *Cytometry Part A* 2009; 75A: 282–288. doi:10.1002/cyto.a.20675
- [25] Stiefel P, Schmidt-Emrich S, Maniura-Weber K, Ren Q. *BMC Microbiol* 2015; 15: 36. doi:10.1186/s12866-015-0376-x
- [26] Ou F, McGovern C, Swift S, Vanholsbeeck F. *Anal Bioanal Chem* 2019; 411: 3653–3663. doi:10.1007/s00216-019-01848-5
- [27] Kasprzycka E, Assunção IP, Bredol M, Lezhnina M, Kynast UH. *J Lumin* 2021; 232: 117818. doi:10.1016/j.jlumin.2020.117818
- [28] Assunção IP, Bredol M, Kasprzycka E, Kynast UH, Lezhnina M. *Inorg Chim Acta* 2021; 515: 120071. doi:10.1016/j.ica.2020.120071
- [29] Greene RA, Slepecky RA. *J Bacteriol* 1972; 111: 557–565. doi:10.1128/jb.111.2.557-565.1972

**Data availability.** The data that support this study are available in the article and accompanying online supplementary material.

**Conflicts of interest.** The authors declare no conflicts of interest.

**Declaration of funding.** WR and UK greatly appreciate the funding granted by the European Union and the State of North Rhine-Westphalia (EFRE OP NRW 2014-2020; Optics Center-R&D). EK, IPA and ML are grateful for support by the German Ministry of Education and Research (BMBF – Bundesministerium für Bildung und Forschung, FKZ I3N14363).

### Author affiliations

<sup>A</sup>Muenster University of Applied Sciences, Institute for Optical Technologies, Stegerwaldstr. 39, 48565 Steinfurt, Germany.

<sup>B</sup>Quantum Analysis GmbH, Mendelstraße 17, 48149 Münster, Germany.

<sup>C</sup>Present address: Faculty of Chemistry, University of Wrocław, 14 F Joliot-Curie Street, 50-383 Wrocław, Poland.

<sup>D</sup>Present address: Instituto Federal de Ciência e Tecnologia (IFSP), Campus Suzano, Avenue Mogi das Cruzes, 1501 Parque Suzano, Suzano, SP, Brazil.